LINEAR TIME VARYING APPROACH TO SATELLITE ATTITUDE CONTROL USING ONLY ELECTROMAGNETIC ACTUATION

Rafał Wiśniewski

Aalborg University, Department of Control Engineering,
Bajers Vej 7, DK-9220 Aalborg Ø, Denmark. raf@control.auc.dk

ABSTRACT

Recently small satellite missions have gained considerable interest due to low-cost launch opportunities and technological improvement of micro-electronics. Required pointing accuracy of small, inexpensive satellites is often relatively loose, within a couple of degrees. Application of cheap, lightweight, and power efficient actuators is therefore crucial and viable. This paper discusses linear attitude control strategies for a low earth orbit satellite actuated by a set of mutually perpendicular electromagnetic coils. The principle is to use the interaction between the Earth's magnetic field and the magnetic field generated by the coils. A key challenge is the fact that the mechanical torque can only be produced in a plane perpendicular to the local geomagnetic field vector, therefore the satellite is not controllable when considered at fixed time. Availability of design methods for time varying systems is limited, nevertheless, a solution of the Riccati equation gives an excellent frame for investigations provided in this paper. An observation that geomagnetic field changes approximately periodically when a satellite is on a near polar orbit is used throughout this paper. Three types of attitude controllers are proposed: an infinite horizon, a finite horizon, and a constant gain controller. Their performance is evaluated and compared in the simulation study of the realistic environment.

INTRODUCTION

The work is motivated by the Ørsted satellite mission. The Ørsted satellite is a 60 kg auxiliary payload scheduled to be launched by a MD-Delta II launch vehicle in the late 1997 into a 450 x 850 km orbit with a 96 degree inclination. The purpose of the Ørsted satellite is to conduct a research program in the discipline of the magnetic field of the Earth. When the satellite is firmly stabilized and the ground contact is established, an $8\ m$ long boom is deployed. The boom carries the scientific instruments that must be displaced from the electro-magnetic disturbances present in the main body of the satellite.

Stabilization of the Ørsted satellite is accomplished by active use of a set of mutually perpendicular coils called magnetorquers. The interaction between external magnetic field of the Earth and the magnetic field generated in the magnetorquers produces a mechanical torque, which is used to correct the attitude. Magnetic control systems are relatively lightweight, require low power and are inexpensive, however they can only be successfully applied for the satellites on high inclined orbits. The Ørsted's coils are mounted in the x, y, and z facets of the main body. A maximum producible magnetic moment is 20 Am^2. The maximum mechanical torque produced by the magnetorquers is approximately $0.6 \cdot 10^{-3}\ Nm$ above the equator, and $1.2 \cdot 10^{-3}\ Nm$ above the Poles.

After boom deployment the nominal operation phase controller is activated. The satellite shall be three axis stabilized with its boom pointing outwards. Formally a coordinate system fixed in the satellite structure shall coincide with a reference coordinate system fixed in orbit. The pointing accuracy is required to be within 10 degrees in pitch, roll, and 20 degrees in yaw.

There is extensive literature covering satellite attitude control design. Most of the algorithms assume application of reaction wheels and/or thrusters for three axis stabilization, though. Attitude control with sole use of magnetorquers has the significant challenge that the system is only controllable in two axes at any time with the axes being perpendicular to the local geomagnetic field vector.

The number of internationally published papers on magnetic attitude control is still rather small. Most of them deal with momentum desaturation of reaction wheel systems. The available literature on magnetorquing for three axis stabilization of satellites includes Reference[1], where a configuration with two magnetic coils and a reaction wheel were analyzed. The problem of three axis control using only electromagnetic coils was addressed in Reference[2]. The local stabilization of the satellite was achieved via implementation of the infinite time horizon linear quadratic regulator. Another linear approach was given in Reference[3], where the linearized time varying satellite motion model was approximated by a linear time invariant counterpart. Three-axis stabilization with use of magnetic torquing of a satellite without appendages was treated in Reference[4], where sliding control law stabilizing a tumbling satellite was proposed. An approach for three-axis magnetic stabilization of a low earth near polar orbit satellite based on Lyapunov theory was presented in Reference[5].

The first part of this study addresses linearization technique for a LEO satellite motion. It is shown that a satellite on a near polar orbit actuated by a set of perpendicular magnetorquers may be considered as a periodic system. In the subsequent sections three types of controllers are design: an infinite horizon, a finite horizon, and a constant gain controller. Their performance is evaluated in the simulation study of the realistic environment.

SATELLITE LINEAR MODEL

The satellite considered in this study is modeled as a rigid body in the Earth gravitational field influenced by the aerodynamic drag torque and the control torque generated by the magnetorquers. The attitude is parameterized by the unit quaternion providing a singularity free representation of the kinematics. The details about mathematical modeling of a LEO satellite can be found in Reference[6]. In this paper only a satellite linear model will be investigated.

It has been already mentioned that the control torque, $\mathbf{N}_{ctrl}$, of the magnetic actuated satellite always lies perpendicular to the geomagnetic field vector, $\mathbf{b}$, furthermore a magnetic moment, $\mathbf{m}$, generated in the direction parallel to the local geomagnetic field has no influence on the satellite motion. This can be explained by the following equality

$$\mathbf{N}_{ctrl} = (\mathbf{m}_{\parallel} + \mathbf{m}_{\perp}) \times \mathbf{b} = \mathbf{m}_{\perp} \times \mathbf{b}, \qquad (1)$$

where $\mathbf{m}_{\parallel}$ is the component of the magnetic moment, $\mathbf{m}$, parallel to $\mathbf{b}$, whereas $\mathbf{m}_{\perp}$ is perpendicular to the local geomagnetic field.

Concluding, the necessary condition for power optimality of a control law is that the magnetic moment lies on a 2-dimensional manifold perpendicular to the geomagnetic field vector.

Consider the following mapping

$$\tilde{\mathbf{m}} \mapsto \mathbf{m} \; : \; \mathbf{m} \; = \; \frac{\tilde{\mathbf{m}} \times \mathbf{b}}{\| \mathbf{b} \|}, \qquad (2)$$

where $\tilde{\mathbf{m}}$ represents a new control signal for the satellite. Now, the magnetic moment, $\mathbf{m}$, is exactly perpendicular to the local geomagnetic field vector and control theory for a system with unconstrained input $\tilde{\mathbf{m}}$ can be applied. The direction of the signal vector $\tilde{\mathbf{m}}$ (contrary to $\mathbf{m}$) can be chosen arbitrary by the controller. From practical point of view, the mapping (2) selects the component of $\tilde{\mathbf{m}}$ which is perpendicular to the local geomagnetic field vector.

The linear model of the satellite motion is given in terms of the angular velocity and the first three components of the attitude quaternion. Linearization of the angular velocity is commonplace and based on the first order extension of the Taylor series. Linearization of the attitude quaternion is quite different due to the multiplicative transformation is needed to describe successive rotations. Consider two rotations, the first one from an orbit fixed coordinate system (OCS) to a reference coordinate system (RCS), the second from RCS to a satellite fixed coordinate system (SCS)

$$\overset{S}{O}\mathbf{q} = \overset{R}{O}\mathbf{q} \, \overset{S}{R}\mathbf{q} \qquad (3)$$

where $\overset{S}{R}\mathbf{q}$, $\overset{R}{O}\mathbf{q}$, $\overset{S}{O}\mathbf{q}$ mean the quaternion mapping RCS to SCS, the quaternion OCS to RCS, and the quaternion transforming OCS to SCS, respectively. $\overset{S}{R}\mathbf{q}$ can be considered as a small perturbation from the reference $[0\ 0\ 0\ 1]^T$. According to Reference[7]

$$\overset{S}{R}\mathbf{q} = \begin{bmatrix} e_1 sin\frac{\delta\phi}{2} \\ e_2 sin\frac{\delta\phi}{2} \\ e_3 sin\frac{\delta\phi}{2} \\ cos\frac{\delta\phi}{2} \end{bmatrix}, \qquad (4)$$

thus for small ϕ

$$\overset{S}{R}\mathbf{q} \approx \begin{bmatrix} \delta q_1 \\ \delta q_2 \\ \delta q_3 \\ 1 \end{bmatrix} \equiv \begin{bmatrix} \delta\mathbf{q} \\ 1 \end{bmatrix}. \qquad (5)$$

As the result, the linearized equation of motion is

$$\frac{d}{dt}\begin{bmatrix} \delta\boldsymbol{\Omega} \\ \delta\mathbf{q} \end{bmatrix} = \mathbf{A}\begin{bmatrix} \delta\boldsymbol{\Omega} \\ \delta\mathbf{q} \end{bmatrix} + \mathbf{B}(t)^c\tilde{\mathbf{m}}, \qquad (6)$$

where

$$\mathbf{A} = \begin{bmatrix} 0 & 0 & 0 & -6\omega_o\sigma_x & 0 & 0 \\ 0 & 0 & \omega_o\sigma_y & 0 & 6\omega_o\sigma_y & 0 \\ 0 & \omega_o\sigma_z & 0 & 0 & 0 & 0 \\ \frac{1}{2} & 0 & 0 & 0 & 0 & 0 \\ 0 & \frac{1}{2} & 0 & 0 & 0 & \omega_o \\ 0 & 0 & \frac{1}{2} & 0 & -\omega_o & 0 \end{bmatrix},$$

$$\sigma_x = \frac{I_y - I_z}{I_x},\ \sigma_y = \frac{I_z - I_x}{I_y},\ \sigma_z = \frac{I_x - I_y}{I_z},$$

$$\mathbf{B} = \begin{bmatrix} \frac{\mathbf{I}^{-1}}{\|\mathbf{b}\|}\begin{bmatrix} -b_y^2 - b_z^2 & b_x b_y & b_x b_z \\ b_x b_y & -b_x^2 - b_z^2 & b_y b_z \\ b_x b_z & b_y b_z & -b_x^2 - b_y^2 \end{bmatrix} \\ \begin{bmatrix} 0 & 0 & 0 \\ 0 & 0 & 0 \\ 0 & 0 & 0 \end{bmatrix} \end{bmatrix},$$

where ω_o is the orbital rate, and I_x, I_y, I_z are components on the diagonal of the inertia tensor $\mathbf{I}$. The matrix $\mathbf{B}(t)$ comes from the double cross product operation $-\mathbf{b}(t) \times (\mathbf{b}(t)\times)$.

Based on the mathematical model provided in this section linear attitude control concepts will be developed. Three controllers will be proposed: an infinite horizon, a finite horizon, and a constant gain controller.

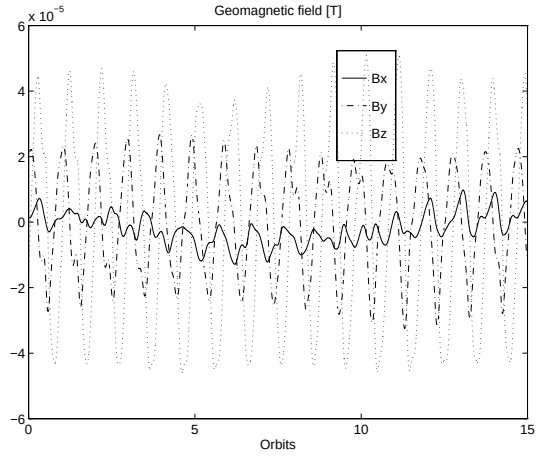

Figure 1: The geomagnetic field vector in RCS propagated by a 10th order spherical harmonic model during 24 h in May 1997.

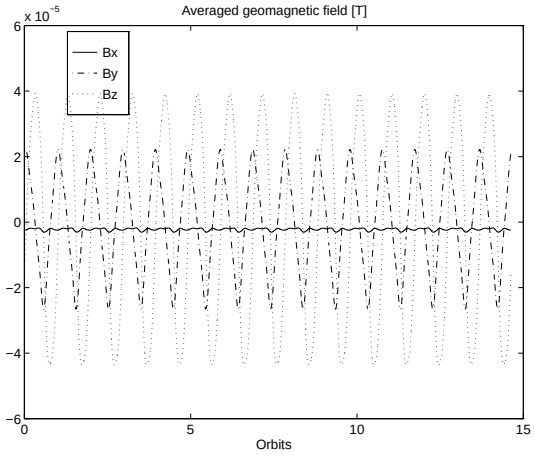

Figure 2: An averaged B-field vector in RCS. Compare with the realistic magnetic field of the Earth in Figure 1 .

INFINITE HORIZON PERIODIC CONTROLLER

The geomagnetic field is essentially that of a magnetic dipole with the largest anomalies over Brazil and Siberia. The geomagnetic field in RCS, has large y and z components, while the x component is comparatively small. The rotation of the Earth is visible via fluctuations of the geomagnetic field vector's x component with frequency $1/24\ 1/hours$, see Figure 1. The following observation is used for the design of an attitude controller. The geomagnetic field on a near polar orbit is approximately periodic with a period $T = 2\pi/\omega_0$.

Due to periodic nature of the geomagnetic field, seen from RCS, the linearized model of the satellite can be considered as periodic. It is though necessary to find an ideally periodic counterpart of the real magnetic field of the Earth. This is done by averaging the geomagnetic field over a time interval reflecting a common period for the satellite revolution about the Earth and the Earth's own revolution. This interval for the Ørsted satellite corresponds to $N = 144$ orbits.

Furthermore, the geomagnetic field is parameterized by the mean anomaly M, since the geomagnetic field and the mean anomaly have the common period T

$$\mathbf{b}_{ave}(M) = \frac{1}{N}\sum_{i=1}^{N}\mathbf{b}(M + i * T). \tag{7}$$

An averaged B-field vector $\mathbf{b}_{ave}(M(t))$ is depicted in Figure 2.

The resultant linear periodic system is

$$\frac{d}{dt}\begin{bmatrix}\delta\mathbf{\Omega}\\ \delta\mathbf{q}\end{bmatrix} = \mathbf{A}\begin{bmatrix}\delta\mathbf{\Omega}\\ \delta\mathbf{q}\end{bmatrix} + \hat{\mathbf{B}}(M)^c\tilde{\mathbf{m}}, \tag{8}$$

where $\hat{\mathbf{B}}(M)$ is given in Eq. (8) after substituting the symbol $\mathbf{B}(t)$ for $\hat{\mathbf{B}}(M)$, and the components of the vector $\mathbf{b}(t)$ for the components of $\mathbf{b}_{ave}(M)$.

The difference between the time varying matrix $\mathbf{B}(t)$ and the ideal periodic counterpart $\hat{\mathbf{B}}(M(t))$ used for the controller design is considered an additional external disturbance torque acting on the satellite.

The controller gain is calculated from the steady state solution of the Riccati equation. According to Theorem 6.3 in Reference[8], if the pair $(\mathbf{A}, \hat{\mathbf{B}}(M))$ is stabilizable then there exists a stabilizing symmetric periodic solution $\mathbf{P}_+(t)$ of the Riccati equation

$$\begin{aligned}-\dot{\mathbf{P}}_+(t) &= \mathbf{P}_+(t)\mathbf{A} + \mathbf{A}^T\mathbf{P}_+(t) \\ &- \mathbf{P}_+(t)\hat{\mathbf{B}}(M)\hat{\mathbf{B}}^T(M)\mathbf{P}_+(t) + \mathbf{Q}.\end{aligned} \tag{9}$$

The periodic solution of the Riccati equation, $\mathbf{P}_+(t)$ is computed from the periodic extension of the steady state solution $\mathbf{P}_\infty(t)$

$$\hat{\mathbf{P}}(t) = \begin{cases}\mathbf{P}_\infty(t) & \text{if } 0 \le t < T\\ \mathbf{0} & \text{otherwise}\end{cases} \tag{10}$$

$$\mathbf{P}_+(t) = \sum_{k=0}^{\infty}\hat{\mathbf{P}}(t - kT). \tag{11}$$

The solution $\mathbf{P}_\infty(t)$ is calculated using backward integration of the Riccati equation for an arbitrary positive definite final condition. This solution converges to the periodic solution. The matrix function $\mathbf{P}_\infty(t)$ corresponding to one orbital passage is stored in the computer memory, and then used for the subsequent orbits.

An example of the periodic matrix function $\mathbf{P}_+(t)$ is illustrated in Figure 3. $\mathbf{P}_+(t_0)$ at fixed time t_0 is a 6 x 6 positive definite matrix. The figure depicts the time history of $P_+(1,1)$, which is typical for the diagonal components. Off-diagonal components change their amplitudes between positive and negative values.

Again, the mean anomaly M can be used for parameterization of $\mathbf{P}_+(M)$, since both $\mathbf{P}_+(t)$ and $M(t)$ are

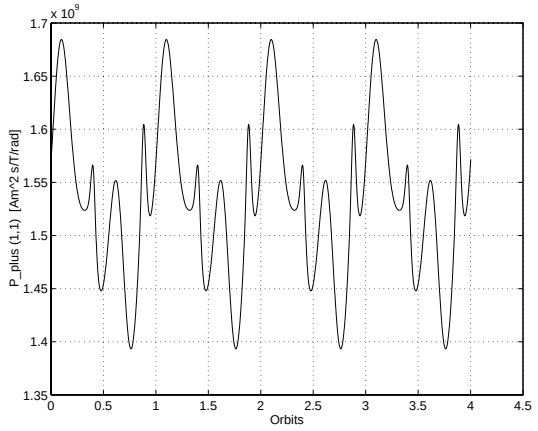

Figure 3: The time history of the (1,1) component of $\mathbf{P}_+$. Notice that $\mathbf{P}_+$ has a period equivalent to the orbit period.

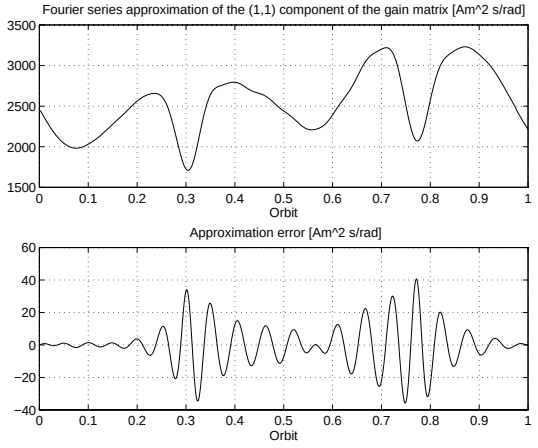

Figure 4: An approximation of the (1,1) component of the gain matrix $\mathbf{K}_+$ by 16th order Fourier series. The discrepancy between $\mathbf{K}_+$ and its Fourier approximation reaches 1.5 per cents at most.

T-periodic. Furthermore, the controller gain matrix is also T-periodic and parameterized with respect to M

$$\mathbf{K}_+(M) = -\mathbf{B}(M)\mathbf{P}_+(M). \tag{12}$$

Implementation

The mean anomaly dependent control gain matrix $\mathbf{K}_+(M)$ is computed off-line and stored in the computer memory. The control signal ${}^c\tilde{\mathbf{m}}(t)$ is then calculated according to

$$\tilde{\mathbf{m}}(t) = \mathbf{K}_+(M) \begin{bmatrix} \Omega_{SR}(t) \\ \mathbf{q}(t) \end{bmatrix}, \tag{13}$$

wehere $\mathbf{\Omega}_{SR}$ is the angular velocity of the satellite relative to RCS, $\mathbf{q}(t)$ is the vector part of the ${}^S_R\mathbf{q}(t)$. Finally, the magnetic moment, ${}^c\mathbf{m}(t)$ is obtained by

$$\mathbf{m}(t) = \frac{\tilde{\mathbf{m}}(t) \times \mathbf{b}(t)}{\| \mathbf{b}(t) \|}. \tag{14}$$

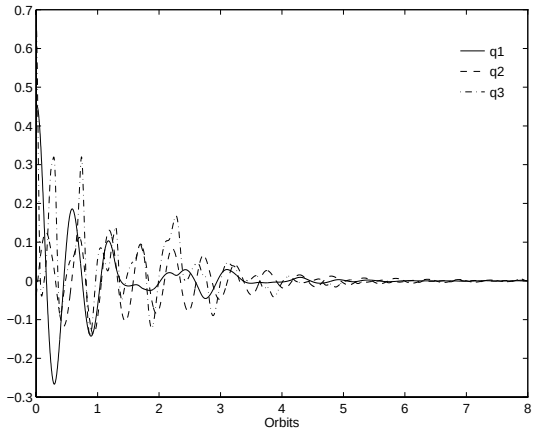

Figure 5: Performance of the infinite horizon controller for a satellite modeled as a linear object. The simulation is carried out for "ideally periodic" geomagnetic field. The initial attitude is $40\ deg$ pitch, $-40\ deg$ roll and $80\ deg$ yaw.

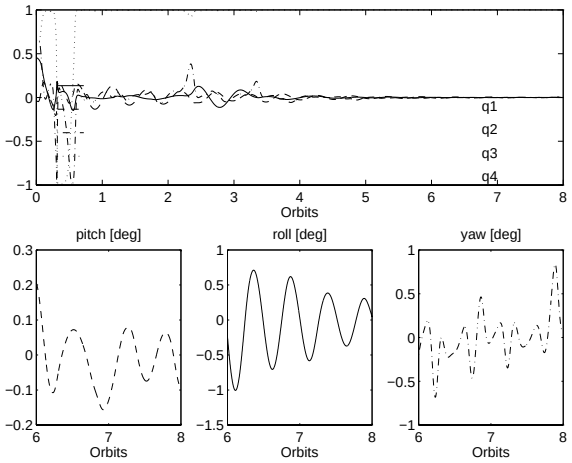

Figure 6: Performance of the infinite horizon controller for the Ørsted satellite on a circular orbit. The initial attitude is the same as in Figure 5. The steady state attitude error is below $1\ deg$.

Another option is to represent $\mathbf{K}_+(M)$ in terms of the Fourier coefficients, benefiting in a reduction of the data stored. A satisfactory approximation of the gain matrix $\mathbf{K}_+$ has been obtained with 16th order Fourier series, see Figure 4. The required capacity of computer memory given in floating point numbers is

$$Memory = \frac{T * No_{elemnts\ in\ \mathbf{K}_+} * Order_{Fourier\ series}}{Sampling\,time}.$$

For example with a sampling time of 10 sec and the orbital period 6000 sec , then 172800 floating point memory is required.

Simulation results of the infinite horizon attitude control are presented in Figure 5, 6 and 7. Figure 5 illustrates performance of the attitude controller for the linear model of the satellite motion with an ideally pe-

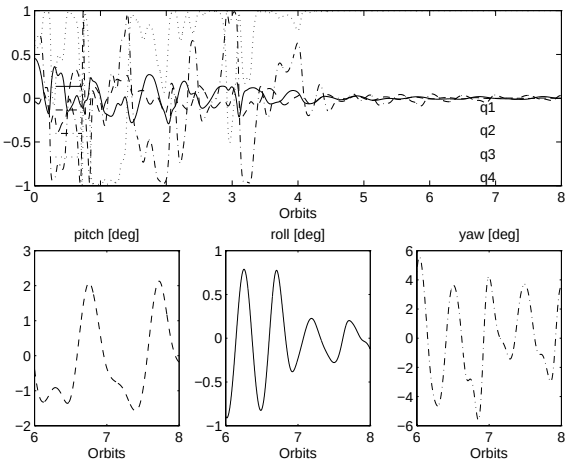

Figure 7: Performance of the infinite horizon controller for the Ørsted satellite on its elliptic orbit. The initial attitude is the same as in Figure 5. The satellite is influenced by the aerodynamic drag for normal solar activity. The attitude error is below 3 deg of pitch and roll. Yaw varies within 6 deg.

riodic geomagnetic field simulator. Figure 6 depicts performance of the infinite horizon attitude controller for the Ørsted satellite in a circular orbit. In Figure 7, the Ørsted satellite is simulated in its elliptic orbit. The satellite motion is affected by the aerodynamic drag for normal solar activity. Additionally, the realistic geomagnetic field is applied in both Figs. 6 and 7.

Disturbances due to eccentricity of the orbit and the aerodynamic drag torque act in the pitch direction. Therefore, both the first component of the quaternion and the first component of the angular velocity, which for small angles correspond to the pitch and pitch rate, are punished slightly more than the remaining components of the state. A diagonal weight matrix $\mathbf{Q}$ with the diagonal $[10\ 6\ 6\ 10\ 6\ 6]^T$ has been implemented for both linear and nonlinear models of the satellite. Initial values of the attitude are the same in both examples corresponding to $40\ deg$ pitch, $-40\ deg$ roll, and $80\ deg$ yaw.

The simulations show that the controller is stable for a wide range of operating points, also very much outside the reference. However, the performance of the infinite horizon controller is relatively poor outside vicinity of the reference, due to influence of the nonlinearities. This can be observed as large variations of the third and fourth component of the attitude quaternion, q_3 and q_4 in Figs. 6 and 7. The result of the disturbance torque due to a difference between the geomagnetic field and its periodic counterpart implemented in the attitude controller is the steady state attitude error in Figure 6. Performance of the infinite horizon attitude controller for the Ørsted satellite affected by the aerodynamic torque is illustrated in Figure 7. The satellite motion is influenced by a moderate aerodynamic drag torque corresponding to normal solar activity. The aerodynamic drag is equal $0.9\ 10^{-5}\ Nm$ at perigee. The attitude error is 3 deg of pitch and roll, whereas yaw angle varies within 6 deg.

A computational expense for the infinite horizon controller lies in the off-line numeric solution to the Riccati equation, but relatively large computer memory is required for keeping the gain data for one orbit. The controller gives a nonzero steady state error also for simulations without external disturbance torques. It is concluded that the infinite horizon magnetic controller is applicable for missions with low pointing requirements. The steady state performance could be improved by the finite horizon controller, which incorporates a realistic model of the geomagnetic field. This type of a control law is discussed in the next section.

FINITE HORIZON PERIODIC CONTROLLER

The linearized model of the satellite motion is only approximately periodic. There is a certain difference between the ideal periodic model of the geomagnetic field developed in the previous section, and the real magnetic field of the Earth. The controller performance could be improved by incorporating the time history of the real geomagnetic field into the controller structure. A new attitude controller based on a transient solution of the Riccati equation is therefore investigated.

The control algorithm is summarized as:

Procedure 1 *1. Calculate the time varying solution of the Riccati differential equation in the time interval* $t \in (\tau - T, \tau]$

$$-\dot{\mathbf{P}}(t) = \mathbf{A}^T\mathbf{P}(t) + \mathbf{P}(t)\mathbf{A} - \mathbf{P}(t)\mathbf{B}(t)\mathbf{B}^T(t)\mathbf{P}(t) + \mathbf{Q}(t) \tag{15}$$

with the final condition

$$\mathbf{P}(\tau) = \mathbf{P}_f. \tag{16}$$

2. Implement controller

$$\tilde{\mathbf{m}}(t) = -\mathbf{B}^T(t)\mathbf{P}(t) \begin{bmatrix} \Omega_{SR} \\ \mathbf{q} \end{bmatrix} \tag{17}$$

for $t \in (\tau - T, \tau]$.

3. Calculate magnetic moment from the equation

$$\mathbf{m}(t) = \frac{\tilde{\mathbf{m}}(t) \times \mathbf{b}(t)}{\| \mathbf{b}(t) \|}.$$

4. τ *becomes* $\tau + T$.

5. go to 1.

It was stated in Reference[6] that if the difference $\mathbf{F} = \mathbf{P}_f - \mathbf{P}(\tau - kT)$ is positive semidefinite for $k \geq 0$ then the procedure given above provides a stable control law (Theorem 3.4.2). The final condition, $\mathbf{P}_f$ is chosen sufficiently large such that $\mathbf{F}$ is positive semidefinite independently on the deviation of the geomagnetic field

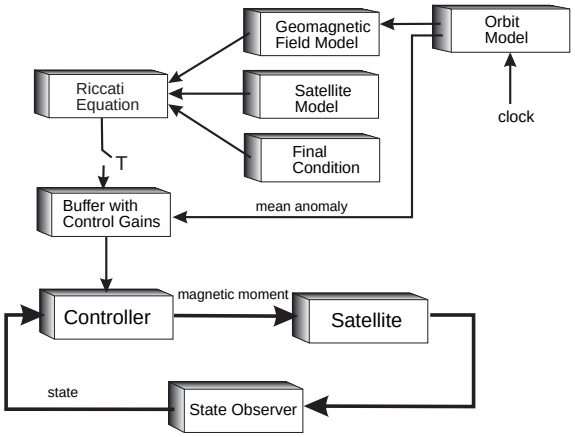

Figure 8: Attitude control system based on finite horizon control.

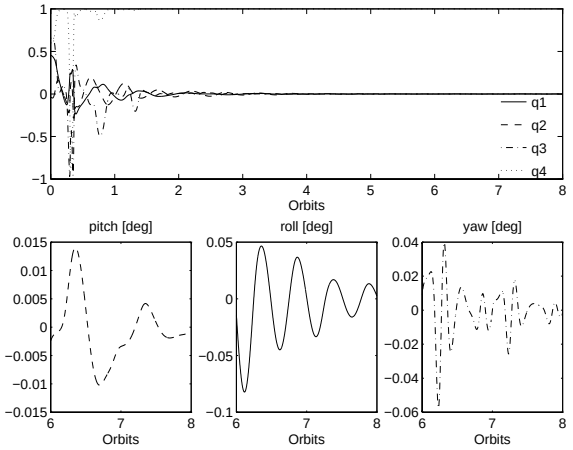

Figure 9: Performance of the quasi periodic receding horizon controller for the Ørsted satellite on circular orbit. The attitude converges asymptotically to the reference, i.e. ${}^{S}_{R}\mathbf{q} \rightarrow [0\,0\,0\,1]^T$.

from its periodic model. It should be noted that the larger $\mathbf{P}_f$, the larger is the control torque. The controller shall comply with the power constraints imposed on the attitude control system, therefore the maximum value of the final condition shall be confined. The final condition is considered as a design parameter, that can be iterated by means of computer simulation.

The attitude control system based on the final horizon control is illustrated in Fig. 8.

The orbit model provides position of the satellite in orbit in terms of longitude, latitude and altitude. This information is used by the on board geomagnetic field model (here 10th order spherical harmonic model). The Riccati equation is computed for the subsequent orbit. The controller gain is computed and parameterized by the mean anomaly. The controller gain is stored in a buffer. This procedure is activated once per orbit. The control gain matrix is taken from the buffer on the basis of the mean anomaly associated with position of the satellite in orbit. The controller gain is updated ev-

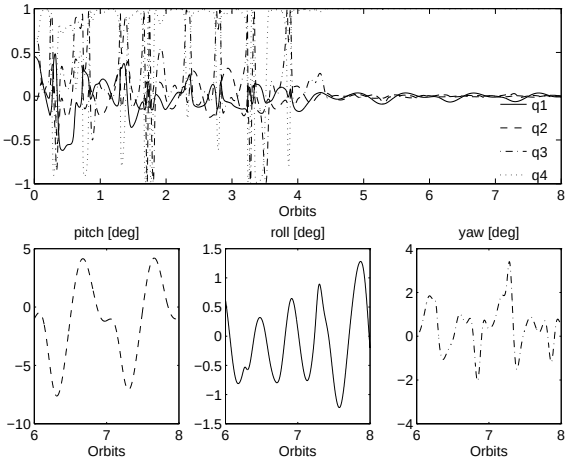

Figure 10: Performance of the quasi periodic receding horizon controller for the Ørsted satellite on the elliptic orbit. The satellite is influenced by the aerodynamic torque. Performance of the receding horizon is comparable with efficiency of the infinite horizon attitude controller in Fig. 7.

ery sampling cycle, and is implemented in the control loop.

Implementation

The quasi periodic receding horizon controller has been validated through computer simulation. The results are depicted in Figs. 9 and 10. Control parameters have been found empirically. Weight matrix $\mathbf{Q}$ has been set to $10\ \mathbf{E}_{6\times 6}{}^{*}$, and the final condition $\mathbf{P}_f$ has been calculated from the steady state solution: $\mathbf{P}_f = \mathbf{P}(\tau) = 2\mathbf{P}_\infty(\tau)$. Initial values of the attitude have again been assigned to $40\ deg$ pitch, $-40\ deg$ roll and $80\ deg$ yaw.

Fig. 9 depicts the Ørsted satellite motion on a circular orbit, i.e. there are no external disturbances. The satellite attitude is seen to converge asymptotically to the reference. The performance of the quasi periodic receding horizon controller for the satellite disturbed by the aerodynamic torque is comparable with the performance of the infinite horizon controller, see Figs. 10 and 7. This is due to the impact of the aerodynamic torque is seen to be much larger than the influence of the torque due to the discrepancy between the geomagnetic field and its periodic counterpart.

The steady state performance of the infinite horizon controller on a circular orbit is much better than infinite horizon, however they are seen to have the same performance for a satellite in an elliptic orbit effected by the aerodynamic drag. The computational burden for the finite horizon controller is heavy due to the Riccati equation shall be solved on board (alternatively uploaded to the on board computer during every ground

* $E_{6\times 6}$ is the 6×6 unit matrix

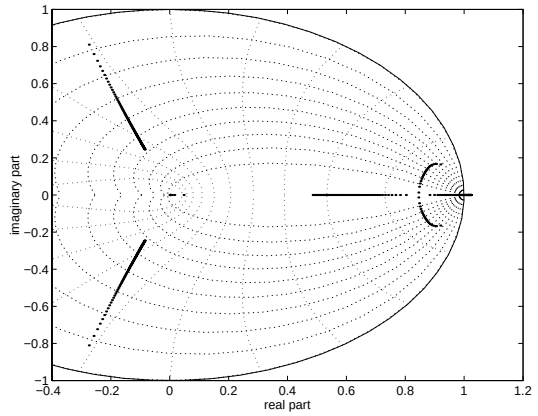

Figure 11: Locus of the characteristic multipliers $\lambda(\epsilon)$ for ϵ changing from 1 to 80 is evaluated for the closed loop system in Eq. (22).The satellite becomes unstable for $\epsilon = 52$, for $\epsilon = 18$ the largest characteristic multiplier is closest to the origin.

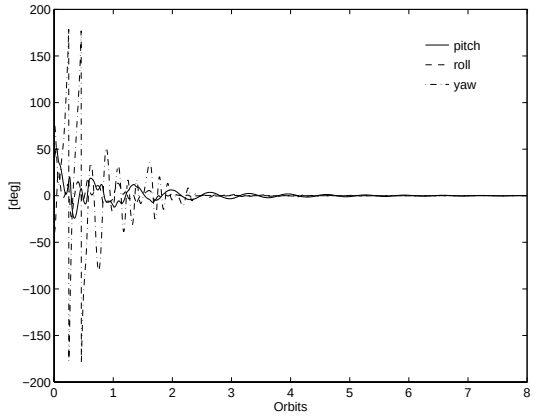

Figure 12: Performance of the constant gain controller for the Ørsted satellite on circular orbit, i.e. without external disturbances. The weigh matrix, $\mathbf{Q}$ has value $18 \cdot \mathbf{E}_{6\times 6}$. Large amplitude of the yaw oscillations is encountered. The initial attitude is $40\ deg$ pitch, $-40\ deg$ roll and $80\ deg$ yaw.

station passage). Therefore, the infinite horizon controller is preferable for the missions like Ørsted with low pointing accuracy. The necessary computer power could be additionally limited if the constant controller was implemented, and had the same performance as the time varying controllers. This issue is addressed in the next section.

CONSTANT GAIN CONTROL

Computation of the infinite and finite horizon attitude controllers are tedious and difficult to implement on a real-time platform. A simple constant gain attitude controller could be an alternative. This type of controller is investigated in this section.

The design algorithm consists of replacing the time varying parameters of the satellite by its averaged values evaluated over a period of one orbit. This concept was first presented in Reference[3]. The theoretical basis of the method was given in Reference[6].

The time invariant counterpart of the time varying linearized satellite motion was

$$\frac{d}{dt}\begin{bmatrix} \delta\mathbf{\Omega} \\ \delta\mathbf{q} \end{bmatrix} = \mathbf{A}\begin{bmatrix} \delta\mathbf{\Omega} \\ \delta\mathbf{q} \end{bmatrix} + \mathbf{B}^c\tilde{\mathbf{m}}, \tag{18}$$

where

$$\mathbf{B} = \frac{1}{T}\int_o^T \hat{\mathbf{B}}(M(t))dt, \tag{19}$$

and T is the orbit period, and $\hat{\mathbf{B}}(M)$ is the control matrix in Eq. (8).

A linear quadratic regulator (LQR) is used for the constant gain controller design. The system is linear, time invariant and controllable thus a control law can be based on the solution of the steady state Riccati equation, see Reference[9]. The optimal control is given by

$$\tilde{\mathbf{m}} = -\mathbf{B}^T\mathbf{P}\begin{bmatrix} \delta\mathbf{\Omega} \\ \delta\mathbf{q} \end{bmatrix}, \tag{20}$$

where $\mathbf{P}$ satisfies the Riccati algebraic equation

$$\mathbf{PA} + \mathbf{A}^T\mathbf{P} - \mathbf{PBB}^T\mathbf{P} + \mathbf{Q} = \mathbf{0}. \tag{21}$$

Once the control vector $\tilde{\mathbf{m}}$ in Eq. (20) is calculated, the magnetic moment, $\mathbf{m}$ is computed according to Eq. (2).

Stability of the control law in Eqs. (20) and (2) for the time varying linear model of the satellite in Eq. (6) is determined using Floquet theory, see Reference[10]. This check is necessary, since stability of the time varying system and its time invariant counterpart are not equivalent. The time invariant system is only the first order approximation of the time varying one, Reference[6]. Furthermore, the sensitivities of those systems are not equivalent neither, e.g. the disturbance torque acting on the satellite in the direction of yaw in a zone near the North nor South poles remains unaffected by the attitude controller (due to lack of controllability), whereas it can be arbitrarily damped by an LQ controller for the time invariant counterpart.

The following closed-loop system is considered for the Floquet analysis

$$\frac{d}{dt}\begin{bmatrix} \delta\mathbf{\Omega} \\ \delta\mathbf{q} \end{bmatrix} = (\mathbf{A} - \hat{\mathbf{B}}^T(M(t))\mathbf{P})\begin{bmatrix} \delta\mathbf{\Omega} \\ \delta\mathbf{q} \end{bmatrix}. \tag{22}$$

As seen from Eqs. (21) and (22) stability of the closed-loop system is dependent on the weight matrix $\mathbf{Q}$. Figure 11 depicts locus of the characteristic multipliers for $\mathbf{Q}(\epsilon) \equiv \epsilon\mathbf{E}_{6\times 6}$, where ϵ changes from 1 to 80 [†]. The

[†] The weight matrix $\mathbf{Q}(\epsilon)$ acts on the state space $[\delta\mathbf{\Omega}\ \delta\mathbf{q}]^T$. $\delta\mathbf{\Omega}$ is provided in rad/s and $\delta\mathbf{q}$ is given without units.

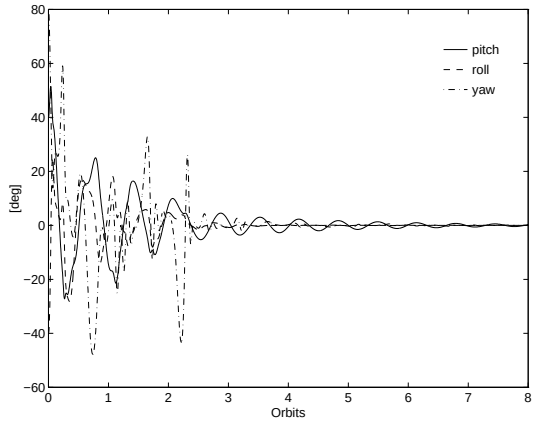

Figure 13: Performance of the constant gain controller for Ørsted satellite on circular orbit. The initial conditions are the same as in Figure 12. The diagonal weight matrix $\mathbf{Q}$ with diagonal $[18\ 18\ 90\ 18\ 18\ 90]^T$ is implemented. The amplitude of the yaw oscillation is reduced comparing with. Figure 12.

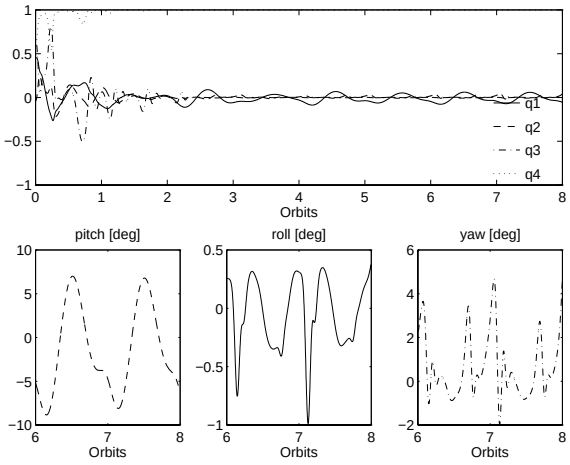

Figure 14: Performance of the constant gain controller for the Ørsted satellite on the elliptic orbit influenced by the aerodynamic drag. The initial conditions are as in Fig. 12. The resultant attitude is within $8\ deg$.

satellite becomes unstable for $\epsilon = 52$. For $\epsilon = 18$, the largest characteristic multiplier is closest to the origin.

Notice that the averaged geomagnetic field is implemented for the Floquet analysis. Therefore, an ultimate test is the simulation for the nonlinear model of the satellite in the realistic space environment.

Validation

The constant gain control demonstrated stability for the entire envelope of the expected satellite initial attitudes and angular velocities in the science observation mission phase. The control parameter: the weight matrix, $\mathbf{Q}$ has been found empirically. Its value has been set to $18 \cdot \mathbf{E}_{6\times 6}$. The simulation results for the Ørsted satellite on the circular orbit in Figure 12 show large amplitude of yaw oscillations. A new diagonal weigh matrix with diagonal $[18\ 18\ 90\ 18\ 18\ 90]^T$ is proposed. The amplitude of the yaw fluctuations is reduced, see Figure 13. The last Figure 14 illustrates the satellite motion on impact of the aerodynamic drag and the torque due to the eccentricity of the Ørsted orbit. The performance of the constant gain controller is very much the same as the infinite and finite horizon attitude controllers in Figs. 7 and 10. The attitude error is within $8\ deg$, which complies with required bond of $\pm 10\ deg$ of pitch and roll, $20\ deg$ of yaw.

CONCLUSION

This paper presented work on the magnetic attitude control based on the steady state and the transient solution of the Riccati equation. It was shown that a satellite on a near polar orbit actuated by a set of perpendicular magnetorquers could be described by a set of periodic differential equations. Three attitude controllers were designed: the finite horizon, the infinite horizon, and the constant gain controller. The control strategies presented were evaluated in the simulation study.

The performance of the designed controllers was comparable for a satellite in an elliptic orbit effected by the aerodynamic drag. The computer expense was smallest for the constant gain controller, therefore it was chosen for on board implementation in the Ørsted satellite. This controller was seen to be stable for a wide envelope of initial values of the attitude, though it had inherently low bandwidth, with time constants on the order of one orbit.

This work is believed to contribute to application of the theory of periodic linear systems to magnetic attitude control problem. It provides solution useful for small satellites with loose requirements on pointing accuracy.

ACKNOWLEDGEMENT

The support of this work by the Danish Ørsted Satellite Project and by the Faculty of Technology and Science at Aalborg University is greatly appreciated.

REFERENCES

1. Cavallo A & al 1993, A sliding manifold approach to satellite attitude control, in *12th World Congress IFAC, Sidney*.

2. Musser K & L Ward 1989, Autonomous spacecraft attitude control using magnetic torquing only, in *Flight Mechanics Estimation Theory Symposium, NASA*.

3. Martel F & al Sep. 1988, Active magnetic control system for gravity gradient stabilized spacecraft, in *Annual AIAA/Utah State University Conference on Small Satellites*.

4. Wisniewski R 1994, Nonlinear control for satellite detumbling based on magnetic torquing, in *Joint Services Data Exchange for Guidance, Navigation, and Control, Arizona*.

5. Wisniewski R & M Blanke Jun. 1996, Three-axis satellite attitude control based on magnetic torquing, in *13th IFAC World Congress, San Francisco, California*.

6. Wisniewski R Dec. 1996, *Satellite Attitude Control Using Only Electromagnetic Actuation*, Ph.D. thesis, Aalborg University.

7. Wertz J 1990, *Spacecraft Attitude Determination and Control*, Kluwer Academic Publishers.

8. Bittanti S, editor 1991, *The Riccati Equation*, Springer Verlag.

9. Kwakernaak H & R Sivan 1972, *Linear Optimal Control Systems*, Wiley.

10. Mohler R 1991, *Nonlinear Systems*, vol. Dynamics and Control, Prentice Hall.